計畫名稱 ： 應用非侵入式故障監測技術於(特)高壓輸電網路供電端監測遠端中(低)壓風場故障位置之判別研究

計畫編號 ： MOST 109-2221-E-228-001

執行單位 ： 明新科技大學 風力發電學士學位學程
主 持 人 ： 章學賢
參與人員 ： 賴澤智

學門歸屬 ： 能源學門

Abstract

The transmission-line fault localization of high-voltage (HV) transmission networks and different medium-voltage (MV) wind farms are implemented using a global time-frequency analysis algorithm, energy-spectrum-based hyperbolic S-transform (HS), to extract the potential power signatures from monitoring non-linear and non-stationary fault signals on HV power utility. An energy concentration algorithm is used to transform each HS coefficient into effective features to quantify various faulty events and reduce recognition algorithms' inputs. Furthermore, the Multiclass classifier processes fault location identification. The simulation results show that the proposed method achieves a high classification rate for considering fault inception angles and fault resistance.

1. Introduction

Wind power is a significant clean energy source due to decreasing petroleum reserves and environmental disruption of carbon emission. To obtain energy from wind power, the regular operation of wind farms is an important issue. The process of obtaining energy is that the wind passes the individual wind turbine, a wind farm component. Therefore, wind energy transfers mechanical kinetic energy into electric power. To effectively use wind power, a substation is needed. It consists of the step-up transformers, power factor correction and voltage control devices, and switching equipment to construct a generation station. Moreover, a large wind farm is usually able to supply over hundreds of megawatts. The amount of power generation is still considerable, though it is smaller than that of all wind turbines' nominal capacity for the overall operating hours in actual conditions.

The present large-scale wind farms may have some potential problems of grid faults, and they may cause the problem of system stability such as transmission-line faults and internal short circuits of the wind turbine. Furthermore, it may lead to blackout occurrences that result in enormous financial losses for users. Hence, finding a method to identify grid faults and enhance the system's stability is excellent urgency. The authors have proposed the best approach for recognizing grid fault types [1]. However, those fault problems usually exist in more than one wind farm in the actual case. Therefore, it will be more difficult and complex to identify the various transmission-line fault locations from high-voltage (HV) transmission networks and numerous medium-voltage (MV) wind farms, especially from monitoring HV power utility.

Many researchers have investigated different protection comparisons and improvements of grid faults for wind farms to enhance the power system's stability [2-7]. Hooshyar et al. [2] revealed distance protection during balanced faults for the transmission lines contacted with the wind farms' induction generator. Deng and Chen [3] proposed a fault ride-through of dc offshore wind farms, which could minimize the transmission system's disturbance between the dc offshore wind farm and the ac grid. Yao et al. [4] suggested an approach to balance a hybrid wind farm capacity between fixed-speed induction generator and permanent magnet synchronous generator when grid faults exist. Kandukuri et al. [5] proposed a scheme to detect and classify wind turbine pitch systems' faults using three-phase motor currents. As mentioned in [5], the extended Park's vector modulus (EPVM) is suitable to diagnose the faults for both permanent magnet synchronous machines (PMSMs) and induction motors (IMs). To find a rapidly real-time scheme of detecting and classifying transmission-line faults for submarine, Wang et al. [6] proposed a method to combine wavelet noise reduction, Clarke transforms, Stockwell transforms (ST), and decision tree (WRC-SDT). Yang et al. [7] analyzed the internal overcurrent faults of the dc transmission systems for the small-scale multi-voltage source converter (VSC) dc wind farms and multi-VSC HV dc (VSC-HVDC) offshore transmission systems.

Furthermore, to overcome HV transmission protection challenges for large-scale wind farms, many works of literature have proposed the protection schemes [8-10]. Pradhan and Joos et al. [8] investigated the protection of lines and studied the trip characteristic for the distance relay. Nayak et al. [9] studied a wide-area protection approach to quickly identify the bus closest to the fault using synchronized phasor measurement units (PMUs). Biswas et al. [10] investigated the impact of transmission lines for the distance relay. They proposed fault detection and classification methods using the sign of the change of positive-sequence currents. As mentioned in [10], the optimization algorithm is significant to minimize the amount of PMUs in wind farms due to the expensive cost and complicated placement of the synchronized PMUs.

Over the years, many researchers have studied the non-intrusive monitoring techniques for home appliances, power distribution systems, and transmission networks [11, 12]. Chang et al. [11] proposed a transient energy method to enhance the non-intrusive load identification accuracy and computational speed. In [11], the authors utilized a turn-on transient characteristic response of home appliances to recognize non-stationary transient signals for each load accurately. Chang et al. [12] proposed an energy spectrum of the wavelet transform (WT) coefficients using Parseval's theorem to represent load turn-on/off transient features without demoting performance.

However, current research shows the methodology of fault location identification of extra-high-voltage (EHV) transmission networks from monitoring power utility sides is not expensive and more accurate recognition [13]. In [13], the authors utilized Parseval's theorem and multiclass support vector machines (SVMs) to quantify different fault locations' energy distribution and obtain fault location identification, respectively. Therefore, a non-intrusive monitoring technique is considered as an alternative scheme for noncommunication protection arrangements.

Figure 1 shows a HV transmission network consisting of the numerous MV wind farms from monitoring the three-phase currents of the HV power utility side. The measured currents are quickly extracted by the proposed non-intrusive fault monitoring (NIFM) scheme to classify the various transmission-line fault locations of HV transmission networks and different MV wind farms. Therefore, the identification results of fault location are employed to analyze power demand zones potentially affected.

This paper's results showed that an uncomplicated and accurate non-intrusive fault localization system is utilized to conquer the problems of non-communication protection schemes and provide a dependable and stable power supply zone. Furthermore, this paper proved the proposed method's identification accuracy has a high success rate by comparing other feature extraction algorithms in electromagnetic transient program (EMTP)/ alternative transients program simulated systems.

This paper is organized as follows: the derivation and presentation of the proposed ES-HS and SVMs are presented in Section II. Section III demonstrates the simulation results for comparisons conducted in this paper. Finally, conclusions are made in Section IV.

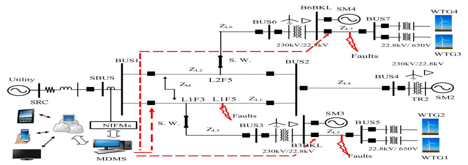

Figure 1. Basic functional scheme of a NIFM sample.

2. Proposed Methods

2.1 Energy Spectrum based HS

S-transform was proposed as the combination of STFT and WT to overcome their drawbacks for transient and nonstationary signals. In fault study, the faulted signals should be fast and accurately detected. It is quietly important to analyze signals in time and frequency domains. At high frequency of fault event, the resolution of symmetrical window is better than that of asymmetrical window. Thus, the generalized window is replaced with a hyperbolic window (*whyp*) to form the generalized HST, i.e.

$$HST(\tau, f) = \int_{-\infty}^{+\infty} x(t) w_{hyp}(\tau - t, f) e^{-i2\pi f t} dt \tag{1}$$

$$w_{hyp} = \frac{2|f|}{\sqrt{2\pi}(\gamma_f + \gamma_b)} e^{\frac{-f^2 V^2}{2}} \tag{2}$$

$$V = \frac{\gamma_f + \gamma_b}{2\gamma_f \gamma_b}(\tau - t - \zeta) + \frac{\gamma_f - \gamma_b}{2\gamma_f \gamma_b}\sqrt{(\tau - t - \zeta)^2 + \lambda^2} \tag{3}$$

where γ_f and γ_b are the parameters of forward-taper and backward-taper, respectively; λ^2 is the positive curvature; and ζ is a translation factor to set the peak of the hyperbolic window at $(\tau\text{-}t)=0$.

In order to determine the discrete HST, discretization of the signal *x(t)* is represented as follows:

$$X(m) = \frac{1}{N}\sum_{m=0}^{N-1} x(k) e^{-i2\pi nk} \tag{4}$$

Then, substituting (4) into (1), one will obtain

$$HST[n, j] = \sum_{m=0}^{N-1} X(m+n) G(m, n) e^{i2\pi mj} \tag{5}$$

The integral of the squared magnitude of a function is known as the energy of the function. A time-frequency signal analysis tool, known as the HST, can improve energy concentration of the ST using a hyperbolic window in the time-frequency domain. A discrete fault signal *s*[n] can be formularized as *S*[K] by the HST, i.e.,

$$HS\_s[n]_{P,L} = S[N]_{P,L} = \begin{bmatrix} S_{1,1} & S_{1,2} & \cdots & S_{1,j} \\ S_{2,1} & S_{2,2} & \cdots & S_{2,j} \\ \vdots & \vdots & \vdots & \vdots \\ S_{i,1} & S_{i,2} & \cdots & S_{i,j} \end{bmatrix}_{P,L} \tag{6}$$

where i is the number of the data samples for each phase P at each location L, and j is the number of scales.

Consequently, through the HST decomposition, the energy of the individual fault transient signal is shown in (7). The term on the right side of (7) denotes the sum of the average power of the decomposed signal.

$$\sum_{n=0}^{K-1} \left| s[n]_{P,L,j} \right|^2 = \frac{1}{K}\sum_{N=0}^{K-1} \left| S[N]_{P,L,j} \right|^2 \tag{7}$$

where K is the total number of the data samples for each scale j.

As stated in the above section, the term in (7), the high-frequency components, will be employed to select the features of fault event in NIFM system. The power spectrum of a fault event signal described by Parseval's Theorem and the HSTCs, the power spectrum of each scale can be obtained as shown in (8). Thus,

$$E_{spectrum} = \left(\frac{1}{I}\sum_{N=0}^{I-1} \left| S[N]_{P,L,j} \right|^2 \right)^{\frac{1}{2}} \tag{8}$$

As demonstrated in Fig. 2, they are the energy spectra of three transmission-line fault locations (Z_{L5}, Z_{L7}, and L1F5) in two MV wind farms and one HV power transmission network, respectively. Accordingly, the distinct energy spectra as the inputs of features for recognition algorithms can effortlessly recognize different transmission-line fault locations.

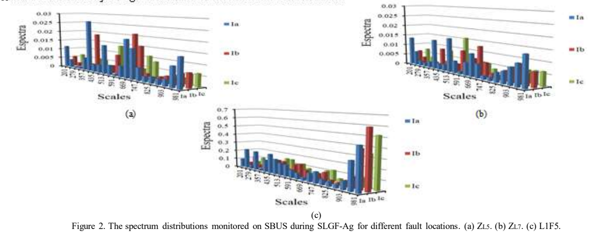

Figure 2. The spectrum distributions monitored on SBUS during SLGF-Ag for different fault locations. (a) Z_{L5}. (b) Z_{L7}. (c) L1F5.

2.2 SVMs

The SVMs are designed as supervised learning algorithms to examine data for classification and regression analyses. To perform classification, SVMs can efficiently operate a nonlinear classification using the nonlinear kernel function for simply mapping their inputs into high-dimensional feature spaces. In the past years, several researchers have applied SVMs to multiclass classification applications. Meyer et al. [16] concluded the SVMs proved very competitive about simple statistical procedures and ensemble methods for classification, mainly yielding good results without the disadvantage of computationally complicated hyperparameter tuning.

To solve multiclass SVM problems, Singh and Shaik [17] utilized two separate SVM models to categorize various induction motor fault problems, i.e., inter-turn shorts of the stator winding and faulty phase detection of phase-to-ground faults. Chang [1] utilized SVM for classifying fault types in a non-intrusive application of HV/EHV power transmission networks.

A library of Support Vector Machines (LIBSVM) utilizes the one-against-one algorithm for multiclass classifications [18]. Fernandez-Delgado et al. [19] studied the SVM classifiers to find that the parameters of LIBSVM, i.e., regularization C and kernel spread gamma, can be automatically tunned to yield the highest average cross-validation accuracy; it is the best SVM classifier with Gaussian kernel function. LIBSVM is used to classify transmission-line fault locations in this paper.

The classification accuracy of LIBSVM is calculated by the following equation (13), i.e.,

$$\text{Classification Accuracy} = \frac{\text{the number of correctly desired data}}{\text{the total number of classification data}} \times 100\% \tag{9}$$

3. Simulation Results

3.1 Study Environment

To implement the non-communication protection scheme of the proposed NIFM, Fig. 1 is an example consisting of two 22.8kV/650V wind farms in a typical three-phase 230kV transmission networks for realizing transmission-line protection implementations by monitoring the HV buses of the power utility side [20].

In Fig. 1, the proposed NIFM system comprises one equivalent power utility source and seven transmission lines. The transmission-line design for L1 and L2 between Bus1 and Bus2 is a mutually coupled double-circuit line. L3, L4, L5, L6, and L7 designed as lumped-parameter models are respectively contacted between L1F3 and Bus3, between Bus2 and Bus4, between B3BKL and Bus5, between L2F5 and Bus6, and between B6BKL and Bus7. There are 72 km long for L1, L2, L3, L4, and L6. There are 3 km long for L5 and L7. Three synchronous motors modeled as the SM2, SM3, and SM4 are contacted with Bus4, Bus3, and Bus6. Two of four doubly-fed induction generators rated 3.88 MVA associate with Bus5 and Bus7 through a step-up transformer. The LIBSVM target outputs of the fault events are located on the node L1F5, Z_{L5}, and Z_{L7}. Finally, different scenarios of fault types such as SLGF, double line-to-ground fault (DLGF), double line fault (DLF), and three-line-to-ground fault (LLLGF) are assigned to examine the achievement for the proposed methods for fault localization.

3.2 Results

The energy-spectrum-based ST (ES-ST) [1], change of the signal energy-based HS (ce-HS) [21], and energy-spectrum-based WT (ES-WT) [12, 22] are employed as benchmark methods for examining the discriminative performance of the proposed ES-HS.

Therefore, ce-HS and ES-WT values are smaller than those of ES-HS and ES-ST from the above results of various fault types in the cross-validation and classification accuracy. The cross-validation accuracy values of ES-HS and ES-ST are above 98.2143% and 98.8095% for various fault types. Moreover, the values of classification accuracy of ES-HS and ES-ST are respectively above 93.9394% and 93.3333% for different fault types.

4. Conclusions

This paper proposes a NIFM system for monitoring the power utility's HV buses to recognize various transmission-line fault locations in the HV transmission networks and different MV wind farms. Unlike PMUs installed on each HV/MV bus, the NIFM system removes intricate communication and synchronization time.

To quantify the HS coefficients for effectively diminishing the input sizes of LIBSVM in this paper, the ES-HS is proposed to form the effective power feature distributions regarding different fault resistances and inception times for each fault type. The acquired results of various fault types show the proposed system is feasible to classify the various transmission-line fault locations in HV transmission networks and different MV wind farms. The classification accuracy can be above 93.9394%.

Acknowledgement

The authors would like to thank the Ministry of Science and Technology, Taiwan, Republic of China for financially supporting this research under Contract No. MOST 109-2221-E-228-001.

References

[1] H. H. Chang, N. V. Linh, and W. J. Lee, "A novel nonintrusive fault identification for power transmission networks using power-spectrum-based hyperbolic s-transform-part I: fault classification", IEEE Trans. Ind. Appl., vol. 54, no. 6, pp. 5700–5710, 2018.
[2] A. Hooshyar, M. A. Azzouz, and E. F. El-Saadany, "Distance protection of lines connected to induction generator-based wind farms during balanced faults", IEEE Trans. Sustain. Energy, vol. 5, no. 4, pp. 1193-1203, 2014.
[3] F. Deng, and Z. Chen, "Operation and control of a dc-grid offshore wind farm under dc transmission system faults", IEEE Trans. Power Del., vol. 28, no. 3, pp. 1356-1363, 2013.
[4] J. Yao, L. Guo, T. Zhou, D. Xu, and R. Liu, "Capacity configuration and coordinated operation of a hybrid wind farm with FSIG-based and PMSG-based wind farms during grid faults", IEEE Trans. Energy Convers., vol. 32, no. 3, pp. 1188-1199, 2017.
[5] S. T. Kandukuri, J. S. L. Senanyaka, V. K. Huynh, and K. G. Robbersmyr, "A two-stage fault detection and classification scheme for electrical pitch drives in offshore wind farms using support vector machine", IEEE Trans. Ind. Appl., 2019, 55, (5), pp. 5109-5118
[6] X. D. Wang, X. Gao, Y. M. Liu, and Y. W. Wang, "WRC-SDT based on-line detection method for offshore wind farm transmission line", IEEE Access, vol. 8, pp. 53547-53560, 2020.
[7] J. Yang, J. E. Fletcher, and J. O'Reilly, "Multi-terminal DC wind farm collection grid internal fault analysis and protection design", IEEE Trans. Power Del., vol. 25, no. 4, pp. 2308-2318, 2010.
[8] A. K. Pradhan and G. Joos, "Adaptive distance relay setting for lines connecting wind farms", IEEE Trans. Energy Convers., vol. 22, no. 1, pp. 206–213, 2007.
[9] P. K. Nayak, A. K. Pradhan, and P. Bajpai, "Wide-area measurement-based backup protection for power network with series compensation", IEEE Trans. Power Del., vol. 29, no. 4, pp. 1970–1977, 2014.
[10] S. Biswas and P. K. Nayak, "A fault detection and classification scheme for unified power flow controller compensated transmission lines connecting wind farms", IEEE Syst. J., vol. 15, no. 1, pp. 297–306, 2021.
[11] H. H. Chang, K. L. Chen, Y. P. Tsai, and W. J. Lee, "A new measurement method for power signatures of nonintrusive demand monitoring and load identification", IEEE Trans. Ind. Appl., vol. 48, no. 2, pp. 764–771, 2012.
[12] H. H. Chang, K. L. Lian, Y. C. Su, and W. J. Lee, "Power-spectrum based wavelet transform for non-intrusive demand monitoring and load identification", IEEE Trans. Ind. Appl., vol. 50, no. 3, pp. 2081-2089, 2014.
[13] H. H. Chang, C. C. Yang, and W. J. Lee, "Fault location identification in power transmission networks using novel non-intrusive fault monitoring systems," IEEE Ind. Appl. Mag., vol. 27, no. 02, pp. 76-89, 2021.
[14] R. G. Stockwell, L. Mansinha, and R. P. Lowe, "Localization of the complex spectrum: the S transform," IEEE Trans. Signal Process., vol. 44, no. 4, pp. 998-1001, Apr. 1996.
[15] A. Ashrafian, M. Rostami, and G. B. Gharehpetian, "Hyperbolic S-transform-based method for classification of external faults, incipient faults, inrush currents and internal faults in power transformers," IET Gener. Trans. Distrib., vol. 6, no. 10, pp. 940-950, Oct. 2012.
[16] D. Meyer, F. Leisch, and K. Hornik, "The support vector machine under test," Neurocomputing, vol. 55, pp. 169-186, 2003.
[17] M. Singh and A. G, Shaik, "Incipient fault detection in stator windings of an induction motor using stockwell transform and SVM," IEEE Trans. Instrum. Meas., vol. 69, no. 12, pp. 9496-9504, Dec. 2020.
[18] C. C. Chang and C. J. Lin, "LIBSVM: a library for support vector machines," ACM Trans. Intell. Syst. Technol., vol. 2, no. 3, pp. 27, Apr. 2011. Software available at http://www.csie.ntu.edu.tw/~cjlin/libsvm
[19] M. Fernandez-Delgado, E. Cernadas, S. Barro, and D. Amorim, "Do we need hundreds of classifiers to solve real world classification problems?" J. Mach. Learn. Res., vol. 15, no. 1, pp. 3133-3181, Jan. 2014.
[20] "EMTP reference models for transmission line relay testing," Power System Relaying and Control Committee, IEEE Power & Energy Society, Sept. 9, 2005. [Online]. Available: https://www.pes-psrc.org/kb/published/reports/EMTP%20Ref%20Model-Final.pdf
[21] S. R. Samantaray, P. K. Dash, and G. Panda, "Fault classification and location using HS-transform and radial basis function neural network," Electr. Power Syst. Res., vol. 76, no. 9-10, pp. 897-905, Jun. 2006.
[22] H. H. Chang, "Non-intrusive fault identification of power distribution systems in intelligent buildings based on power-spectrum-based wavelet transform," Energy Build., vol. 127, pp. 930-941, Sept. 2016.

TABLE I. CLASSIFICATION RESULTS OF SLGF-AG

Method	ES-HS	ES-ST	ce-HS	ES-WT
Accuracy in Cross Validation (%)	99.8909	99.8363	97.3268	75.7774
Accuracy in Classification (%)	100	100	96.8852	73.1694
C	32768.0	32768.0	32768.0	32768.0
Gamma	2.0	8.0	8.0	8.0
Aver. Cross Validation Time (s)	38.7643	43.4063	55.5962	31.1861
Aver. Classification Time (s)	0.19701	0.2427	0.19521	0.15884

TABLE II. CLASSIFICATION RESULTS OF SLGF-BG

Method	ES-HS	ES-ST	ce-HS	ES-WT
Accuracy in Cross Validation (%)	99.8909	99.6727	96.9995	73.868
Accuracy in Classification (%)	99.9454	99.9454	97.1585	70.929
C	32768.0	32768.0	32768.0	2048.0
Gamma	2.0	8.0	8.0	8.0
Aver. Cross Validation Time (s)	39.50462	44.27177	56.38523	30.91718
Aver. Classification Time (s)	0.19319	0.197546	0.191514	0.149178

TABLE III. CLASSIFICATION RESULTS OF SLGF-CG

Method	ES-HS	ES-ST	ce-HS	ES-WT
Accuracy in Cross Validation (%)	100	99.9454	98.1997	72.6132
Accuracy in Classification (%)	100	99.8907	97.4317	70.1639
C	32768.0	32768.0	32768.0	8192.0
Gamma	2.0	8.0	8.0	2.0
Aver. Cross Validation Time (s)	38.72754	44.33445	52.72778	31.11944
Aver. Classification Time (s)	0.195609	0.204355	0.183143	0.151673

TABLE IV. CLASSIFICATION RESULTS OF SLGF-ABCG

Method	ES-HS	ES-ST	ce-HS	ES-WT
Accuracy in Cross Validation (%)	100	100	100	94.599
Accuracy in Classification (%)	100	100	100	95.082
C	8.0	128.0	32.0	32768.0
Gamma	0.5	0.5	0.5	8.0
Aver. Cross Validation Time (s)	30.48816	33.48727	39.43831	33.90692
Aver. Classification Time (s)	0.189264	0.217007	0.197668	0.12678